Analysis and Pumping of the Albedo Function

László Neumann, Attila Neumann, László Szirmay-Kalos *
Department of Control Engineering and Information Technology,
Technical University of Budapest
Budapest, Műegyetem rkp. 11, H-1111, HUNGARY
szirmay@fsz.bme.hu

Technical Report TR-186-2-98-20
Institute of Computer Graphics, Vienna University of Technology

Abstract: The paper introduces a method, called the albedo pumping-up, to derive new, physically plausible BRDFs from an existing one or from any symmetric function. This operation can be applied recursively by arbitrary number of times. An important application of this operation is the transformation of the Phong and Blinn models in order to make them produce metallic effects. The paper also examines the albedo function of reflectance models and comes to the conclusion that widely used models violate energy balance at grazing angles.

Keywords: Reflectance function, BRDF representation, albedo function, energy balance, metal models, perceptual based fitting

1 Introduction

In computer graphics the optical material properties are usually modeled by reflectance models that are defined by BRDFs. Intuitively, the BRDF represents the radiance reflected off the material illuminated by point lightsources from a given direction.

The most famous BRDF model that can describe specular materials was proposed by Phong [Pho75] and improved by Blinn [Bli77]. This model does not have physical interpretation but is only a mathematical construction. Since the original forms violate physics (they are not symmetric), their corrected versions [ICG86][Lew93] are preferred in global illumination algorithms.

The first model that has physical base was proposed by Torrance and Sparrow [TS66], which was applied in rendering algorithms in [CT81]. Later, He, Torrance et. al. [HTSG91] introduced another model that even more accurately represented the underlying physical phenomena [BS63]. These models are not suitable for importance sampling since it would require the integration and inversion of the probability density functions that are expected to be proportional to the reflected power. Not only is it impossible to compute the required integral and inversion analytically, but even the calculation of BRDF values requires significant computational effort for these physically based models. In their recent paper Lafortune et. al. approximated a non-linear, metallic BRDF by the sum of modified Phong models [LFTG97]. The resulting BRDF is simple, but this approach requires a great number of elementary terms to sufficiently represent highly specular materials at grazing angles.

Radiosity and Monte-Carlo ray-tracing rendering algorithms require that the BRDFs do not violate physics. Such shading models must satisfy both reciprocity and energy balance, and are called *physically plausible* [Lew93].

*This work has been supported by the National Scientific Research Fund (OTKA), ref.No.: F 015884, the Austrian-Hungarian Action Fund, ref.No.: 29ö4, 32öu9 and the Spanish-Hungarian Action Fund, ref.No.: E/9.

Reciprocity that was recognized by Helmholtz is the symmetry property of the BRDF (f_r, $[\mathrm{sr}^{-1}]$), which is defined by the following equation [Min41]:

$$f_r(\mathbf{L}, \mathbf{V}) = f_r(\mathbf{V}, \mathbf{L}), \tag{1}$$

where $\mathbf{L}$ is the unit vector pointing towards the incoming light and the unit vector $\mathbf{V}$ defines the viewing direction. Several rendering algorithms, including ray-tracing, takes advantage of this symmetry property.

Suppose that the surface is illuminated by a beam from direction $\mathbf{L}$. *Energy balance* means that the *albedo*, that is the fraction of the total reflected power, cannot be greater than 1:

$$a(\mathbf{L}) = \int_{\Omega} f_r(\mathbf{L}, \mathbf{V}) \cdot \cos\Theta_{\mathbf{V}} \, d\omega_{\mathbf{V}} \leq 1. \tag{2}$$

Energy balance makes the linear operator of the rendering equation or some of its powers [NN95] a contraction, which is usually required by iterative and random walk methods to converge to the solution. Particularly, the albedo together with occlusion conditions determine the norm of the integral operator and consequently the conditioning of the rendering equation, and thus describe the speed of convergence of the iterative methods, and can be used to specify how many light bounces are to be computed during random walks.

1.1 Perceptual based fitting

The albedo and the BRDF characterize a material in two different aspects. The BRDF expresses the *radiance reflectivity* of the material — that is the response to point lightsources —, while the albedo describes its *energy reflectivity* and is responsible to the response for uniformly distributed (so called *sky-light*) illumination. Concentrated point-like and uniformly distributed lightsources represent the two extreme cases of possible illuminations.

Formally, if a surface is illuminated by a point lightsource of power 4π at distance 1 in direction $\mathbf{L}$, then the observer at direction $\mathbf{V}$ will perceive:

$$L^{\mathrm{out}}(\mathbf{V}) = f_r(\mathbf{L}, \mathbf{V}) \cdot \cos\Theta_{\mathbf{L}}. \tag{3}$$

On the other hand, if the illumination is constant in all directions and its radiance is 1, then the perceived radiance is:

$$L^{\mathrm{out}}(\mathbf{V}) = \int_{\Omega} f_r(\mathbf{L}, \mathbf{V}) \cdot \cos\Theta_{\mathbf{L}} \, d\omega_{\mathbf{L}} = a(\mathbf{V}). \tag{4}$$

Since perception is affected by both point lightsources (sun, electric bulbs) and sky-light illumination (sky, diffuse room, large area lightsources), in order for a reflectance model to be realistic, both the BRDF weighted by the cosine factor and the albedo should accurately follow the corresponding characteristics of the real materials. So far, fitting has been made only on the the BRDF using usually least square error metric. In perceptual based fitting the albedo should also be considered, and the maximal relative errors of both the weighted BRDF and of the albedo should be minimized simultaneously. The relative error corresponds to the logarithmic characteristics of the human vision system.

1.2 Physically plausible, but not physically based models

Let us consider the specular part of the original versions of the Phong [Pho75] and Blinn [Bli77] models. Using the widely accepted notations where $\mathbf{R}$ is the mirror direction of $\mathbf{L}$, $\mathbf{N}$ is the unit normal vector, and $\mathbf{H}$ is the halfway unit vector between $\mathbf{L}$ and the view vector $\mathbf{V}$, the Phong and Blinn models are

defined as the nth power of the dot products $(\mathbf{RV})$ and $(\mathbf{NH})$, respectively, divided by the cosine of the incident angle.

$$\begin{aligned} f_{r,\mathrm{Phong}}(\mathbf{L},\mathbf{V}) &= c_{\mathrm{Phong}}(n)(\mathbf{R}\cdot\mathbf{V})^n/\cos\Theta_{\mathbf{L}}, \\ f_{r,\mathrm{Blinn}}(\mathbf{L},\mathbf{V}) &= c_{\mathrm{Blinn}}(n)(\mathbf{N}\cdot\mathbf{H})^n/\cos\Theta_{\mathbf{L}}. \end{aligned} \tag{5}$$

These models are not symmetric because of the division by $\cos\theta_{\mathbf{L}}$, and thus are not physically plausible. A simple way of making them physically plausible is the elimination of this division [Lew93], resulting in the following versions:

$$\begin{aligned} f'_{r,\mathrm{Phong}}(\mathbf{L},\mathbf{V}) &= c_{\mathrm{Phong}}(n)(\mathbf{R}\cdot\mathbf{V})^n, \\ f'_{r,\mathrm{Blinn}}(\mathbf{L},\mathbf{V}) &= c_{\mathrm{Blinn}}(n)(\mathbf{N}\cdot\mathbf{H})^n. \end{aligned} \tag{6}$$

The Lafortune model [LFTG97] also falls into this category, but uses a special type of dot product:

$$f_{r,\mathrm{Lafortune}}(\mathbf{L},\mathbf{V}) = c_{\mathrm{Lafortune}}(n,s)(\mathbf{R}_x\mathbf{V}_x + \mathbf{R}_y\mathbf{V}_y + s\mathbf{R}_z\mathbf{V}_z)^n \tag{7}$$

where $c_{\mathrm{Phong}}(n)$,$c_{\mathrm{Blinn}}(n)$, $c_{\mathrm{Lafortune}}(n,s)$ are scalar functions of material constants.

For large n values the BRDF gets highly specular. However, the Phong and Blinn models cannot provide metallic or mirror looking since as the incident angle grows towards the grazing angle, the ratio of the reflected power as well as the output radiance decrease. If n goes to infinity, then the reflected radiance and the albedo converges to zero for 90 degree incident angle since in this limit case the albedo follows the cosine function. Intuitively, the decrease of the radiance means that if we look at a Phong-mirror, then the image reflected in the mirror gets darker for greater reflection angles (the non-plausible versions do not exhibit this darkening). Note that Lafortune's model tries to reduce this phenomenon by using a factor s to suppress the BRDF close to perpendicular angles and thus giving an emphasis to grazing angles.

2 Analysis of the energy reflectivity of classical BRDF models

The energy balance of the reflectance models can be represented by their albedo function. Supposing that the Fresnel term is 1 (for silver this is practically true), the albedos of the Phong, He-Torrance, Cook-Torrance and the Ward [War92] models are shown in figure 1. Note that the Cook-Torrance and the Ward models diverge at grazing angles, while the Phong, He-Torrance and Ward BRDFs badly decrease for greater incident angles. Since shiny metals tend to be good energy mirrors even for larger incident angles, the decrease of the albedo for larger incident angles makes a model not realistic for representing metallic objects.

The divergent behavior of the Cook-Torrance and the Ward models was quite unexpected, since these models have been believed to be physically plausible, and this type of divergence may generate incorrect results and may cause instability when rendering special scenes. This kind of divergence is caused by the application of $\mathbf{H}$ instead of $\mathbf{R}$ in the reflectance model. Models of type $\mathbf{N}\cdot\mathbf{H}$ cannot effectively separate viewing directions that are close to the mirror direction and therefore the size of the solid angle of the highlight cannot shrink depending on $\mathbf{L}$. For grazing angles the BRDF should converge to a dirac-delta like shape (the value of BRDF goes to infinity, while the albedo should be limited), but the not sufficient shrinking of the support of the highlight does not allow that. The following section formally examines this phenomenon.

2.1 Divergence of the Cook-Torrance and Ward models

Let us denote the angle between the normal vector and the halfway vector by δ, and the surface roughness parameter by m. The BRDF function of the Ward model [War92] is

$$f_{r,\mathrm{Ward}}(\mathbf{L},\mathbf{V}) = \frac{1}{4\pi m^2}\cdot\exp\left(-\tan^2\delta/m^2\right)\cdot\frac{1}{\sqrt{(\mathbf{N}\cdot\mathbf{L})(\mathbf{N}\cdot\mathbf{V})}}, \tag{8}$$

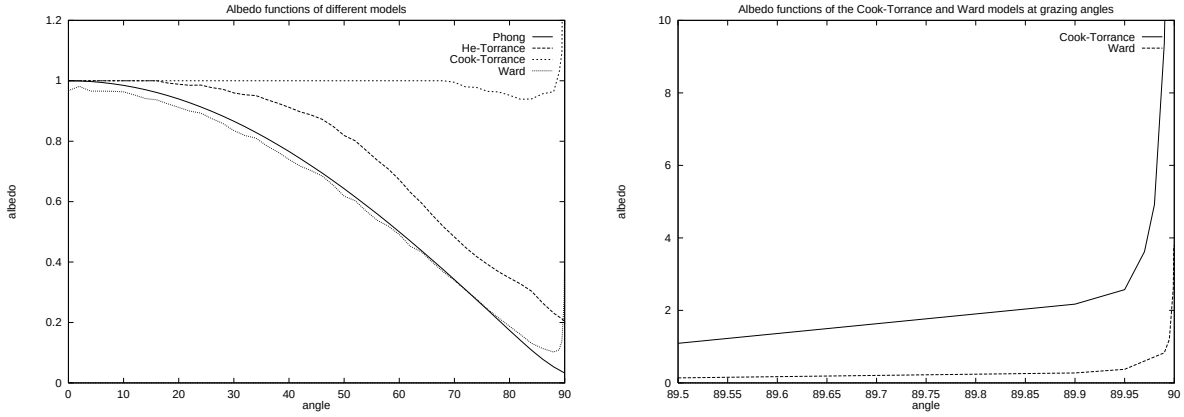

Figure 1: Albedo functions of the Phong ($n = 150$), He-Torrance ($\sigma_0 = 0.1,\ \tau = 1.7$), Cook-Torrance ($m = 0.1$) and Ward ($m = 0.1$) models

Assuming that the Fresnel factor is 1, the BRDF of the Cook-Torrance model [CT81] is

$$f_{r,\mathrm{Cook}}(\mathbf{L},\mathbf{V}) = \frac{1}{4\pi m^2 \cos^4\delta} \cdot \exp\left(-\tan^2\delta/m^2\right) \cdot \frac{G(\mathbf{N},\mathbf{L},\mathbf{V})}{(\mathbf{N}\cdot\mathbf{L})(\mathbf{N}\cdot\mathbf{V})}, \tag{9}$$

where the *geometry factor* G [SKe95] is

$$G(\mathbf{N},\mathbf{L},\mathbf{V}) = \min\{2\cdot\frac{(\mathbf{N}\cdot\mathbf{H})(\mathbf{N}\cdot\mathbf{V})}{(\mathbf{V}\cdot\mathbf{H})}, 2\cdot\frac{(\mathbf{N}\cdot\mathbf{H})(\mathbf{N}\cdot\mathbf{L})}{(\mathbf{L}\cdot\mathbf{H})}, 1\}. \tag{10}$$

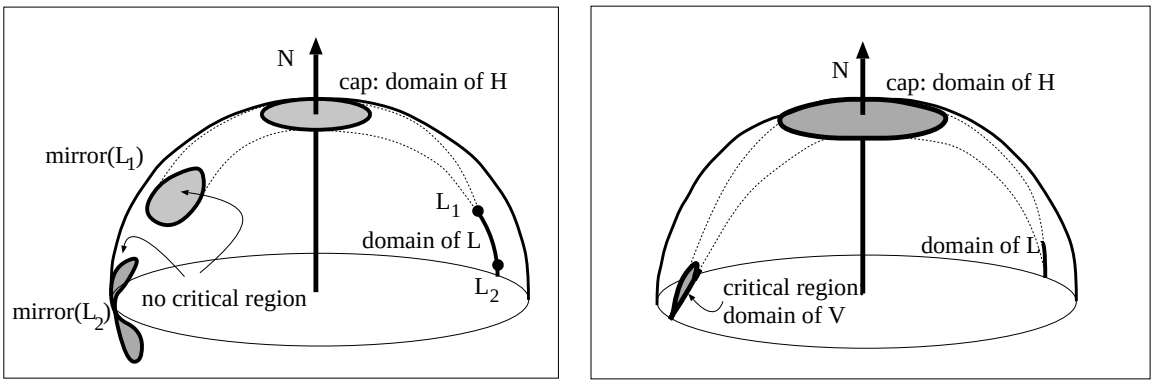

Figure 2: The relations between the domains of $\mathbf{L}$, $\mathbf{H}$ and $\mathbf{V}$ vectors (left figure: domain of $\mathbf{L}$ is too big compared to the domain of $\mathbf{H}$; right figure: domain of $\mathbf{L}$ is small compared to the domain of $\mathbf{H}$)

Let us consider the situation around the highlight close to the grazing angles, that is where $\mathbf{V} \approx \mathbf{R}$, $\mathbf{H} = (\mathbf{L}+\mathbf{V})/|\mathbf{L}+\mathbf{V}| \approx \mathbf{N}$, $\mathbf{N}\cdot\mathbf{L} \approx 0$ and $\mathbf{N}\cdot\mathbf{V} \approx 0$. We have to show that it is possible to move $\mathbf{L}$ towards grazing angles in a way that the albedo will diverge along this path. An appropriate path is a sufficiently small arc of the main circle of the directional hemisphere. For a given vector $\mathbf{L}$, the albedo integral requires the consideration of all vectors $\mathbf{V}$. However, establishing a lower bound, only those viewing vectors are considered which, together with $\mathbf{L}$ result in those $\mathbf{H}$ halfway vectors that are inside a *cap* (spherical circle around $\mathbf{N}$) (figure 2). Since $\mathbf{H} = (\mathbf{L}+\mathbf{V})/|\mathbf{L}+\mathbf{V}|$ should hold, the allowable domain of viewing vectors $\mathbf{V}$ can be determined from these two regions by "spherical mirroring" of each

point in the domain of $\mathbf{L}$ onto each point in the domain of $\mathbf{H}$. The left figure demonstrates that if the domain of $\mathbf{L}$ is too big compared to that of $\mathbf{H}$, then those $\mathbf{V}$ vector sets which correspond to different $\mathbf{L}$ vectors will not have a common intersection. However, if the domain of $\mathbf{L}$ is small compared to that of $\mathbf{H}$, then the $\mathbf{V}$ vector sets corresponding to different $\mathbf{L}$ vectors will have a common intersection (right figure 2). This region of intersection constrained to the the upper hemisphere is called the *critical region.*

In the Ward model, factor $(1/4\pi m^2) \cdot \exp\left(-\tan^2\delta/m^2\right)$ can be lowerbounded inside the *cap*, so can the $(1/4\pi m^2\cos^4\delta) \cdot \exp\left(-\tan^2\delta/m^2\right)$ factor of the Cook-Torrance model. Thus we can find appropriate positive constants μ_{Ward}, and μ_{Cook} so that

$$\frac{1}{4\pi m^2} \cdot \exp\left(-\tan^2\delta/m^2\right) \geq \mu_{\mathrm{Ward}},$$

$$\frac{1}{4\pi m^2\cos^4\delta} \cdot \exp\left(-\tan^2\delta/m^2\right) \geq \mu_{\mathrm{Cook}}. \tag{11}$$

Considering the geometry term and the denumerator of the Cook-Torrance model, we can further restrict the domain of $\mathbf{L}$ and the *cap* for $\mathbf{H}$ to guarantee that the constant 1 is the real minimum in the geometry term, thus here we can apply the following substitution

$$\frac{G(\mathbf{N},\mathbf{L},\mathbf{V})}{(\mathbf{N}\cdot\mathbf{L})(\mathbf{N}\cdot\mathbf{V})} = \frac{1}{(\mathbf{N}\cdot\mathbf{L})(\mathbf{N}\cdot\mathbf{V})}. \tag{12}$$

Using the constant lower bounds valid inside the *cap*, we can obtain:

$$\frac{\mu_{\mathrm{Ward}}}{\sqrt{(\mathbf{N}\cdot\mathbf{L})(\mathbf{N}\cdot\mathbf{V})}} \leq f_{r,\mathrm{Ward}}(\mathbf{L},\mathbf{V}),$$

$$\frac{\mu_{\mathrm{Cook}}}{(\mathbf{N}\cdot\mathbf{L})(\mathbf{N}\cdot\mathbf{V})} \leq f_{r,\mathrm{Cook}}(\mathbf{L},\mathbf{V}). \tag{13}$$

For the albedo, a lowerbound can be established by bounding the hemispherical domain Ω to the *critical region* $\Omega_{\mathrm{critical}}$ and using inequality (13). Let us consider the Ward model:

$$a_{\mathrm{Ward}}(\mathbf{L}) \geq \int\limits_{\Omega_{\mathrm{critical}}} \frac{\mu_{\mathrm{Ward}}}{\sqrt{(\mathbf{N}\cdot\mathbf{L})(\mathbf{N}\cdot\mathbf{V})}} \cdot (\mathbf{NV})\, d\omega_{\mathbf{V}} = \frac{\mu_{\mathrm{Ward}}}{\sqrt{(\mathbf{N}\cdot\mathbf{L})}} \int\limits_{\Omega_{\mathrm{critical}}} \sqrt{(\mathbf{N}\cdot\mathbf{V})}\, d\omega_{\mathbf{V}}. \tag{14}$$

For the albedo of the Cook-Torrance model, we can obtain:

$$a_{\mathrm{Cook}}(\mathbf{L}) \geq \int\limits_{\Omega_{\mathrm{critical}}} \frac{\mu_{\mathrm{Cook}}}{(\mathbf{N}\cdot\mathbf{L})(\mathbf{N}\cdot\mathbf{V})}(\mathbf{N}\cdot\mathbf{V})\, d\omega_{\mathbf{V}} = \frac{\mu_{\mathrm{Cook}}}{(\mathbf{N}\cdot\mathbf{L})} \cdot |\Omega_{\mathrm{critical}}|. \tag{15}$$

Since at grazing angles $(\mathbf{NL})$ converges to zero, the lowerbounds in equations (14) and (15) diverge, which forces the albedo of the Ward and Cook-Torrance models to diverge as well.

3 Albedo pumping-up

Examining the albedo functions of the plausible Phong and Blinn models, we can realize that they are two small for higher incident angles, thus they cannot provide, for example, metallic appearance. If we could find an operation that is not too complicated and preserves reciprocity and energy balance of a known BRDF model, but increases its albedo, then the application area of these models could be significantly widened.

We propose the following operation, which starts with an arbitrary, but symmetric BRDF $f_r(\mathbf{L},\mathbf{V})$, or with a symmetric function, and corrects this as follows to obtain a new BRDF:

$$f_r^*(\mathbf{L},\mathbf{V}) = \frac{f_r(\mathbf{L},\mathbf{V})}{g(\mathbf{L},\mathbf{V})}, \tag{16}$$

where we require function g to be a symmetric function of $\mathbf{L}$ and $\mathbf{V}$, and also

$$\max(a(\mathbf{L}), a(\mathbf{V})) \leq g(\mathbf{L}, \mathbf{V}) \leq 1 \tag{17}$$

to hold.

Note that even if the original BRDF is only symmetric, but is not energy preserving, then the first pumping-up operation makes it energy preserving and thus physically plausible.

Assume that function g is not zero (except for a set of null measure). Since $g(\mathbf{L}, \mathbf{V}) \leq 1$, we obtain $a^*(\mathbf{L}) \geq a(\mathbf{L})$ for the albedo a^* of $f_r^*(\mathbf{L}, \mathbf{V})$. Furthermore, if for some of the directions $g(\mathbf{L}, \mathbf{V}) < 1$, then $a^*(\mathbf{L})$ is definitely greater than $a(\mathbf{L})$. Consequently, equation (16) increases the albedo, which justifies our name "*pumping-up*".

The new BRDF is obviously symmetric, thus only the energy conservation must be proven to demonstrate that the pumped-up model is also physically plausible.

The albedo of $f_r^*(\mathbf{L}, \mathbf{V})$ is

$$a^*(\mathbf{L}) = \int_\Omega \frac{f_r(\mathbf{L}, \mathbf{V})}{g(\mathbf{L}, \mathbf{V})} \cdot \cos\Theta_\mathbf{V} \, d\omega_\mathbf{V} \leq \int_\Omega \frac{f_r(\mathbf{L}, \mathbf{V})}{\max(a(\mathbf{L}), a(\mathbf{V}))} \cdot \cos\Theta_\mathbf{V} \, d\omega_\mathbf{V} =$$

$$\frac{1}{a(\mathbf{L})} \int_\Omega f_r(\mathbf{L}, \mathbf{V}) \cdot \cos\Theta_\mathbf{V} \, d\omega_\mathbf{V} + \int_{\Omega_\mathbf{V}} f_r(\mathbf{L}, \mathbf{V}) \cdot \left(\frac{1}{a(\mathbf{V})} - \frac{1}{a(\mathbf{L})}\right) \cos\Theta_\mathbf{V} \, d\omega_\mathbf{V} \leq 1. \tag{18}$$

where $\Omega_\mathbf{V}$ contains those directions for which $\max(a(\mathbf{L}), a(\mathbf{V})) = a(\mathbf{V})$.

In order to realize that the albedo is less than 1, let us consider the sum of the last two terms. The integral of the first term is $a(\mathbf{L})$, thus the complete first term equals to 1. Since in $\Omega_\mathbf{V}$, factor $(1/a(\mathbf{V}) - 1/a(\mathbf{L}))$ is negative, the second integral is negative and thus the albedo is less than 1. Summarizing, we obtain:

$$a(\mathbf{L}) \leq a^*(\mathbf{L}) \leq 1. \tag{19}$$

The set $\Omega_\mathbf{V}$ is empty only if $a(\mathbf{L}) = 1$, which results in $a^*(\mathbf{L}) = 1$. Since real materials absorb some energy, albedo pumping-up always increases the albedo.

Equation (16) can also be used recursively several times, which generates a monotonically increasing sequence of albedo functions. In order to make the evaluation of the pumped-up BRDF fast during rendering, the albedo should be precomputed and stored in a one-variate table.

3.1 Definition of the correction term

We examine two alternatives for the definition of correction term g and analyze their effect on the Phong and Blinn models.

First, let the correction term be

$$g_1(\mathbf{L}, \mathbf{V}) = \max(a(\mathbf{L}), a(\mathbf{V})). \tag{20}$$

This function obviously satisfies inequality (17).

The effects of this type of pumping-up on the Phong and Blinn models are shown in figure 3 and figure 4, respectively. Note that the albedos resulted by recursive pumping-ups converge to the albedo of the ideal mirror (constant 1).

It is also worth examining the output radiance assuming a single point-like lightsource of intensity 4π at distance 1 in direction $\mathbf{L}$. In this case the irradiance is $\cos\Theta_\mathbf{L}$. The output radiances of the pumped-up Phong and Blinn models at different incident directions are shown in figure 3 and figure 4, respectively. These figures demonstrate that the "Phong and Blinn mirrors" get darker for greater incident angles, but the pumping-up reduces this effect. However, after several pumping-up operations the output radiance can significantly exceed the received irradiance. This means that for certain viewing directions the mirror

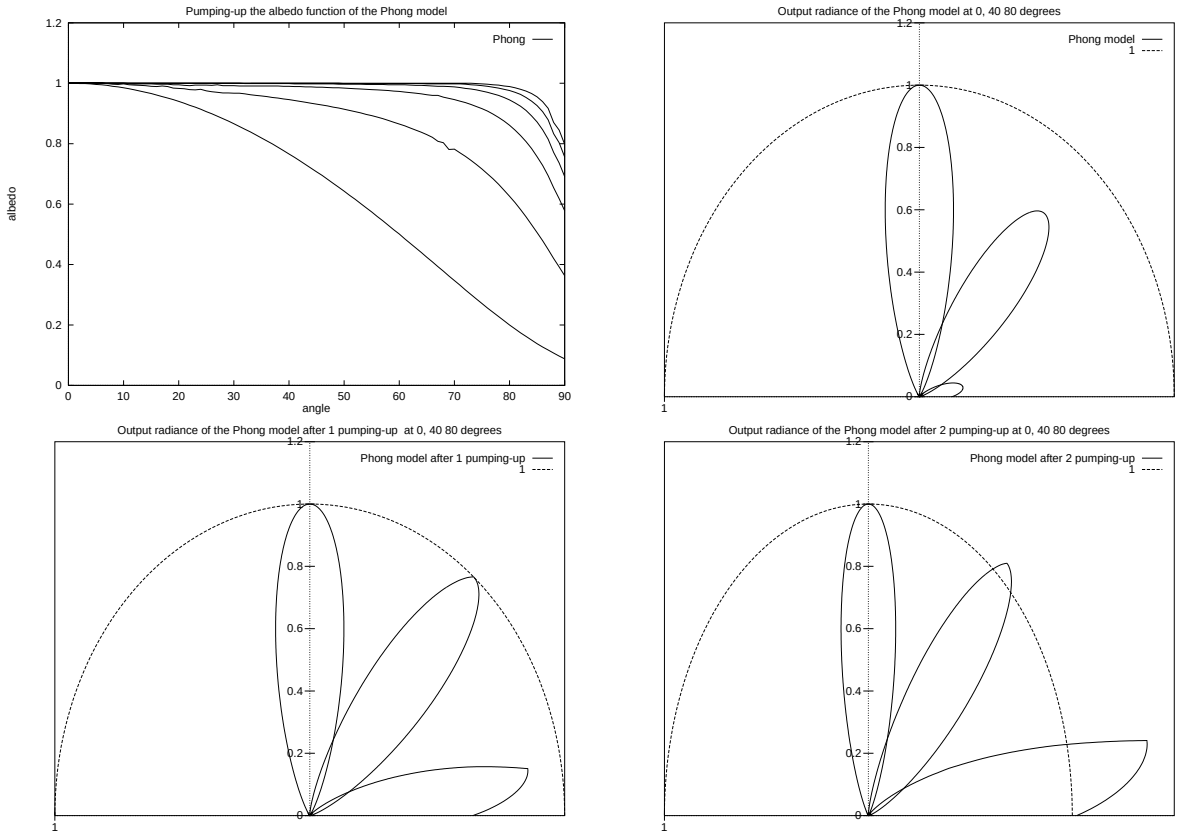

Figure 3: Albedo and reflected radiance of the reciprocal Phong model and its pumped-up versions (n=20)

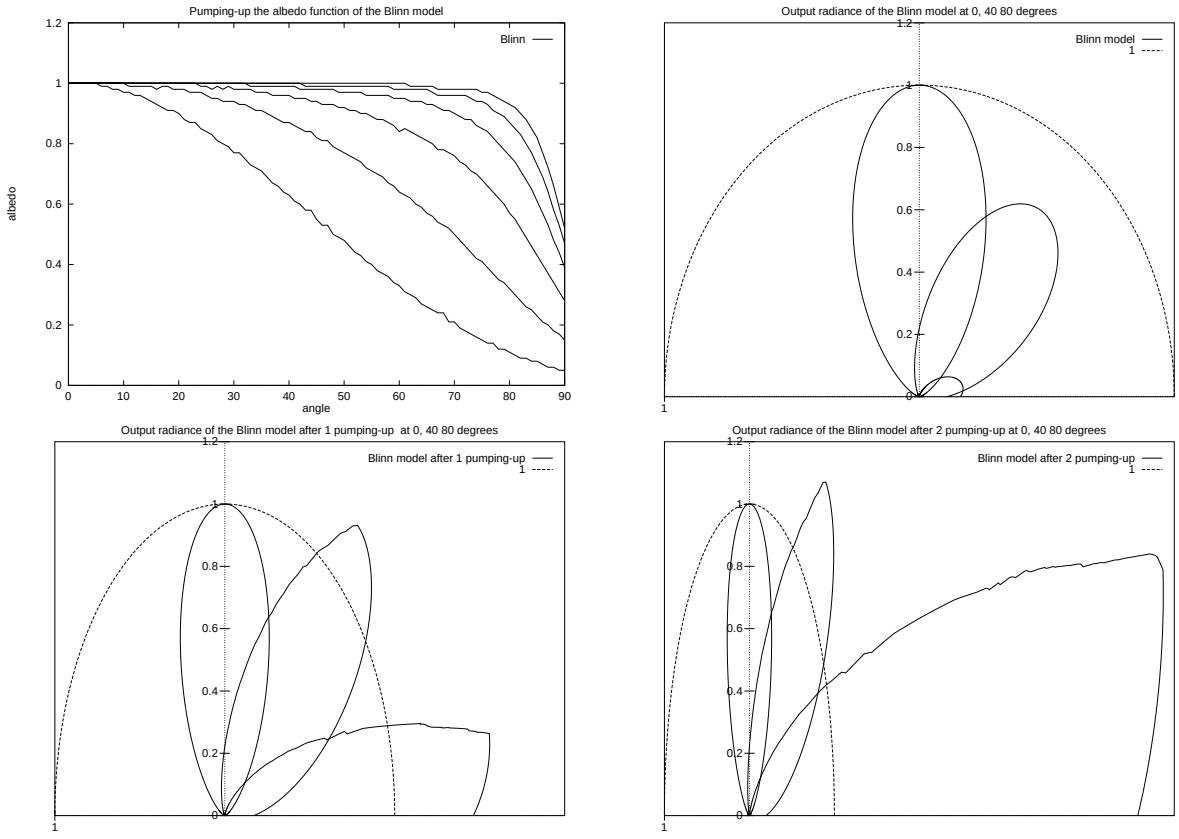

Figure 4: Albedo and reflected radiance of the reciprocal Blinn model and its pumped-up versions ($n = 20$)

image is brighter than the original one. This phenomenon can be observed on rough metals and is called the *off-specular peak.* However, if this effect is too strong, then the image will be unrealistic.

This artifact can be eliminated by the "*controlled albedo pumping-up*" that is discussed by the following section.

3.2 Controlled albedo pumping-up

In order to control the radiance at grazing angles, another correction term is chosen:

$$g_2(\mathbf{L}, \mathbf{V}) = \max(a(\mathbf{L}), a(\mathbf{V}), (\mathbf{N} \cdot \mathbf{V}), (\mathbf{N} \cdot \mathbf{L})). \tag{21}$$

Since the dot products are not greater than 1, function g_2 also meets requirement (17).

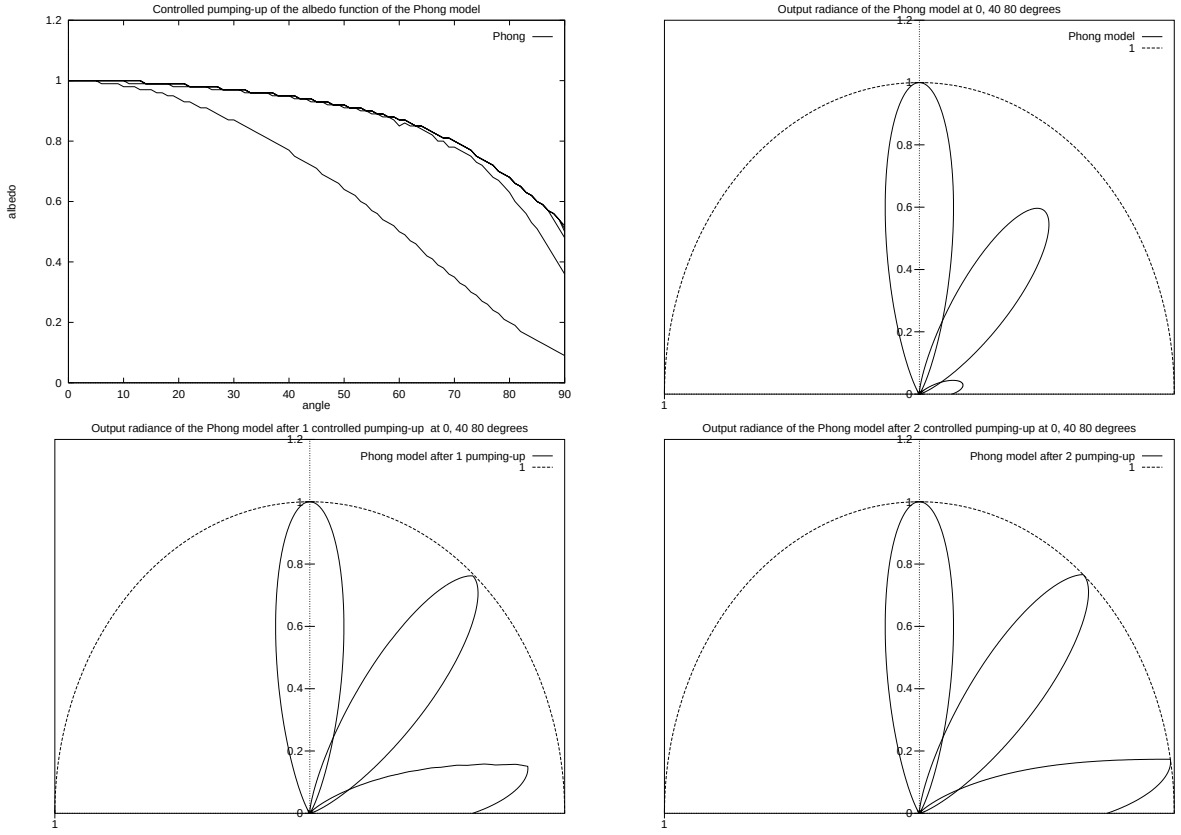

Figure 5: Controlled pumping-up of the reciprocal Phong model ($n = 20$)

The albedos and the output radiances of the Phong and the Blinn models after controlled pumping-up are shown in figure 5 and in figure 6, respectively.

Note the this type of controlling also has its price. Namely, the perfect energy mirror cannot be generated using many recursive pumping-up operations. The process will converge to an albedo that is below the constant 1. Note that for $n = 20$, the Phong model is worth pumping-up 2 or 3 times, but the albedo of the Blinn model does not significantly increase with the second and consecutive pumping-up operations.

The limitation of the output-radiance and the increase of the albedo are two contradicting objectives. If we optimize for one, then the other will get farther from its desired shape. Since the Phong model's lobes are thinner, it is better in redistributing bigger power response if the albedo is pumped-up.

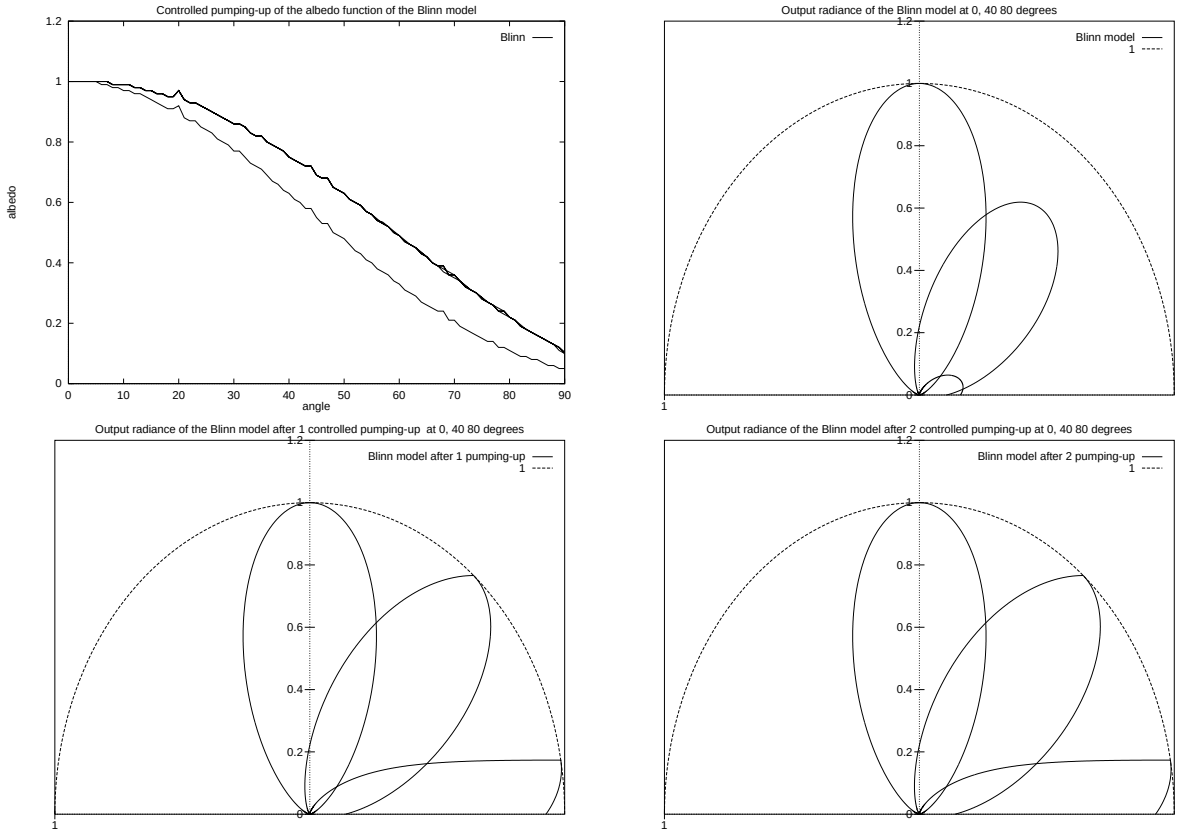

Figure 6: Controlled pumping-up of the reciprocal Blinn model ($n = 20$)

If we consider the repetition of the controlled pumping-ups of the Phong model, an interesting observation can be made. The final, pumped-up BRDF can also be obtained in the following, very simple form:

$$f_r(\mathbf{L}, \mathbf{V}) = c_n \cdot \frac{(\mathbf{R} \cdot \mathbf{V})^n}{\max((\mathbf{N} \cdot \mathbf{L}), (\mathbf{N} \cdot \mathbf{V}))}. \tag{22}$$

where $c_n \leq (n+2)/2\pi$ must hold in order for the model to preserve energy balance.

The albedo functions of different exponents n and the output radiance of this *new model* are shown in figure 7.

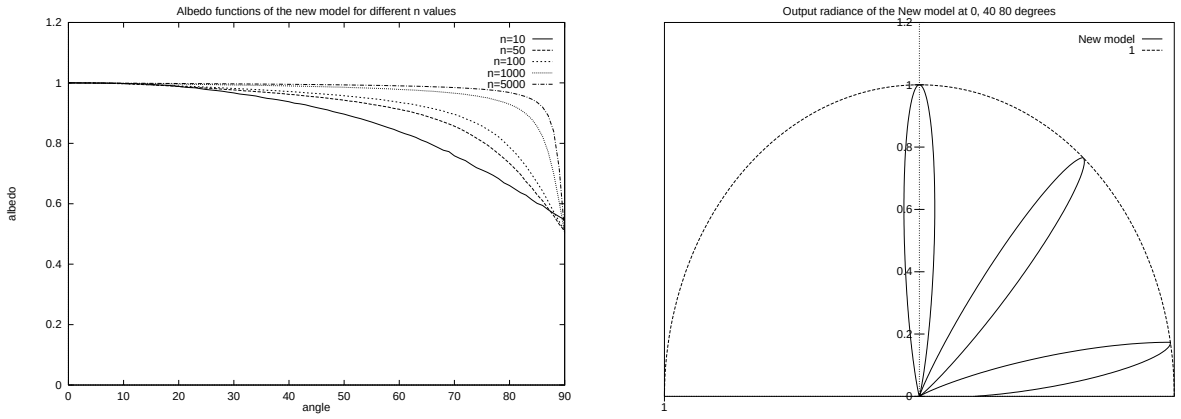

Figure 7: The albedo function for different n parameters and the output radiance ($n = 100$) of the new model

4 Simulation results

The following images have been rendered by Monte-Carlo ray-tracing method applying importance sampling. Color computation was carried out at 8 discrete wavelengths, then using the color matching functions the XYZ primaries were generated, which were finally converted to RGB. The material properties of the metals (index of refraction and extinction coefficient), color matching functions and the XYZ to RGB conversion matrix were taken from [Gla95].

Figure 8 show images of metallic objects, rendered with the reciprocal Phong and its pumped-up reflection models, using $n = 20$ and $n = 5000$ exponent parameters. The scene is illuminated by both point lightsources and sky-light. Note that pumping-up makes the image brighter and also more metallic looking. Images of $n = 5000$ demonstrate that the original Phong model is a bad energy mirror, since the sky-light illumination cannot make the surfaces bright where the angle of viewing is large. However, pumping-up eliminates this problem.

5 Conclusions

The paper presented a method to control and tune the shape of the albedo function, which is called the "albedo pumping-up". The operation can be applied recursively. Albedo pumping-up can improve the energy response without violating the physical plausibility.

The elaboration of this operation was inspired by the need to make the Phong and Blinn models appropriate for metallic objects. The original Phong and Blinn BRDFs are "dark" for greater incident angles from two different aspects. On the one hand, the output radiance converges to zero. On the other hand, the fraction of the total reflected energy also converges to zero if the exponents of these

models go to infinity when approximating highly specular materials. These models are poor radiance-mirrors and energy-mirrors at grazing angles. Our intention was to improve the albedo function by the introduced pumping-up operation to get a better "energy-mirror", and hoped that it also results in a good "radiance-mirror". This worked well for the Phong model, but the Blinn model showed super-metal characteristics even for moderate increase of the albedo function (the output radiance of super-metals significantly exceeds the input radiance and the allowed size of the off-specular peak). In order to limit the output radiance, we introduced the *controlled albedo pumping-up*, which guarantees that the output radiance does not exceed the input radiance, but it also drastically limited the increase of the albedo for the Blinn model.

Based on these experiences, other reflectance models of the $\mathbf{N} \cdot \mathbf{H}$ family have been analyzed to find out how they tried to compromise these two contradicting objectives. The analysis and the numerical simulations resulted in an unexpected conclusion that the Ward and the Cook-Torrance models violate energy balance and their albedos diverge to infinity at grazing angles, thus these models are not physically plausible. We believe that the $\mathbf{N} \cdot \mathbf{H}$ family is not appropriate for the construction of metallic BRDFs. Their albedos either badly decrease (Blinn model) or diverge (Ward and Cook-Torrance models) at grazing angles.

The albedo is not an abstract feature of a material but can be seen directly. The perceived radiance reflected of an object illuminated by uniform distributed light is just proportional to the albedo function at the viewing direction if the BRDF is reciprocal. This phenomenon is also demonstrated by the color images, where the albedo pumping-up improved not only the highlights but also the parts affected only by the sky-light illumination and viewed at large angles.

In order to emphasize the role of the albedo, the *perceptually based fitting* was proposed, which fits both the BRDF (response to point lightsources) and the albedo (response to sky-light) simultaneously to find minimal relative error. The application of relative error metric is justified by the logarithmic characteristics of the perception. This type of fitting requires the storage of the albedo functions in addition to BRDFs in material databases. The albedo can be measured by integrating sphere or using distributed lighting.

References

[Bli77] James F. Blinn. Models of light reflection for computer synthesized pictures. In *Computer Graphics (SIGGRAPH '77 Proceedings)*, pages 192–198, 1977.

[BS63] Petr Beckmann and Andre Spizzichino. *The Scattering of Electromagnetic Waves from Rough Surfaces.* MacMillan, 1963.

[CT81] R. Cook and K. Torrance. A reflectance model for computer graphics. *Computer Graphics*, 15(3), 1981.

[Gla95] A. Glassner. *Principles of Digital Image Synthesis.* Morgan Kaufmann Publishers, Inc., San Francisco, 1995.

[HTSG91] X. He, K. Torrance, F. Sillion, and D. Greenberg. A comprehensive physical model for light reflection. *Computer Graphics*, 25(4):175–186, 1991.

[ICG86] D. S. Immel, M. F. Cohen, and D. P. Greenberg. A radiosity method for non-diffuse environments. In *Computer Graphics (SIGGRAPH '86 Proceedings)*, pages 133–142, 1986.

[Lew93] R. Lewis. Making shaders more physically plausible. In *Rendering Techniques '93*, pages 47–62, 1993.

[LFTG97] E. Lafortune, S. Foo, K. Torrance, and D. Greenberg. Non-linear approximation of reflectance functions. *Computer Graphics (SIGGRAPH '97 Proceedings)*, pages 117–126, 1997.

[Min41] M. Minnaert. The reciprocity principle in lunar photometry. *Astrophysical Journal*, 93:403–410, 1941.

[NN95] L. Neumann and A. Neumann. Radiosity and hybrid methods. *ACM Transactions on Graphics*, 14(3):233–265, 1995.

[ON94] M. Oren and S. Nayar. Generalization of lambert's reflectance model. *Computer Graphics (SIGGRAPH '94 Proceedings)*, pages 239–246, 1994.

[PF90] P. Poulin and A. Fournier. A model for anisotropic reflection. *Computer Graphics*, 24(4):273–281, 1990.

[Pho75] Bui Thong Phong. Illumination for computer generated images. *Communications of the ACM*, 18:311–317, 1975.

[SKe95] L. Szirmay-Kalos (editor). *Theory of Three Dimensional Computer Graphics.* Akadémia Kiadó, Budapest, 1995.

[TS66] K. Torrance and M. Sparrow. Off-specular peaks in the directional distribution of reflected thermal distribution. *Journal of Heat Transfer — Transactions of the ASME*, pages 223–230, May 1966.

[War92] G. Ward. Measuring and modeling anisotropic reflection. *Computer Graphics*, 26(2):265–272, 1992.

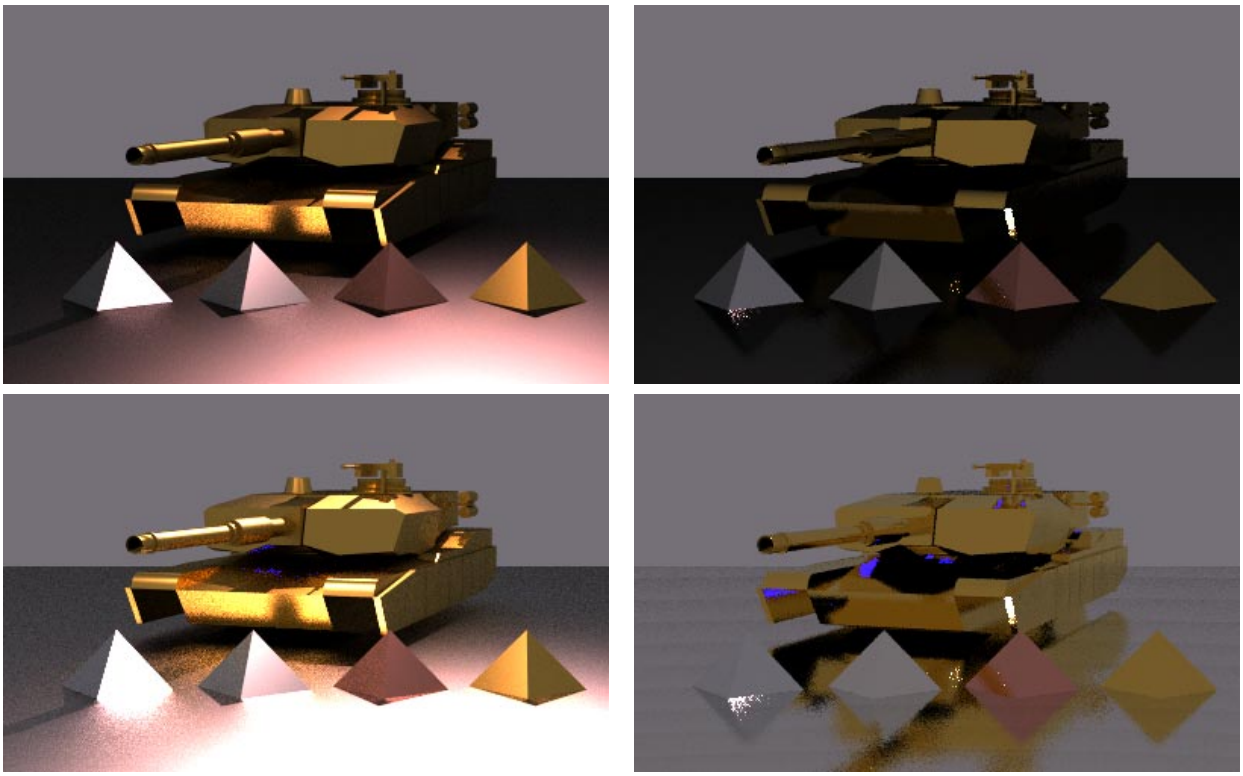

Figure 8: A golden tank with aluminum, silver, copper and golden pyramids rendered using the reciprocal Phong model (top) and using the Phong model pumped-up once (bottom) (left: $n = 20$, right: $n = 5000$)